



1 Research on Hydrogeochemical Characteristics and Transformation Relationships 2 between Surface Water and Groundwater in the Weihe River

3 Jihong Qu¹, Shibao Lu^{2,*}, Zhipeng Gao^{3,1}, Wujin Li^{4,1}, Zhiping Li¹, Furong Yu¹

4 (1 School of Resources and Environment, North China University of Water Resources and Electric Power, Zhengzhou 450045, China

5 2 School of Public Administration, Zhejiang University of Finance and Economics, Hang Zhou 310018, China;

6 3 School of Water Resources and Environment, China University of Geosciences (Beijing), Beijing 100083, China

7 4 Guangdong Hydropower Planning and Design Institute, Guangzhou 510635, China)

8 *corresponding author: Lu5111284@aliyun.com

9
10 **Abstract:** The transforming relationship between surface water and groundwater as well as their origins are the basis for studying the
11 transport of pollutants in river-groundwater systems. A typical section of the river was chosen to sample the surface water and
12 shallow groundwater. Then, a Piper trilinear diagram, Gibbs diagram, ratios of major ions, factor analysis, cluster analysis and other
13 methods were used to investigate the hydrogeochemical evolution of surface water and groundwater and determine the formation of
14 hydrogeochemical components in different water bodies. Based on the distribution characteristics of hydrogen and oxygen stable
15 isotopes δD and $\delta^{18}O$ and discharge hydrograph separation methods, the relationship between surface water and groundwater in the
16 Weihe River was analyzed. The results indicated that the river water is a $SO_4 \cdot Cl - Na$ type and that the groundwater
17 hydrogeochemical types are not the same. The dominant anions are HCO_3^- in the upstream reaches and are SO_4^{2-} and Cl^- in
18 downstream reaches. Hydrogeochemical processes include evaporation and concentration, weathering of rocks, ion exchange, and
19 dissolution infiltration reactions. The δD and $\delta^{18}O$ of surface water change little along the river and are more enriched than are those
20 of the groundwater. With the influences of precipitation, irrigation, river recharge and evaporation, the δD and $\delta^{18}O$ of shallow
21 groundwater at different sections are not the same. There is a close relationship between the surface water and groundwater. Surface
22 water supplies the groundwater, which provides the hydrodynamic conditions for the entry of pollutants into the aquifer.

23 **Keywords:** hydrogeochemical characteristics; hydrogen and oxygen stable isotopes; surface water-groundwater system; cycle and
24 transformation

25 26 1. Introduction

27 The regularity of the water cycle and the conversion between surface water and groundwater is the basis for
28 the study of pollutant transport in river-groundwater systems (Lu et al., 2016a; Shang et al., 2017). Different water
29 bodies have different hydrogeochemical characteristics and isotopic signatures because of their different sources
30 of recharge, environments and circulation conditions. Hence, hydrogeochemical characteristics are the ideal
31 tracers for tracking water circulation processes. Analyses of hydrogeochemical and isotopic characteristics of
32 rivers and groundwater can effectively reveal the relationship in the transformation of river water to groundwater.

33 Descriptive statistics, graphic analysis and multivariate statistical analysis are used to analyze the
34 hydrogeochemical characteristics (Lu et al., 2015). Graphic methods include the Durov diagram, Stiff diagram,
35 Piper diagram and Gibbs diagram. Common multivariate statistical analysis methods include factor analysis
36 (Keesari et al., 2016), principal component analysis (Chattopadhyay and Singh, 2103) and cluster analysis (Zhang
37 et al., 2012). Stable isotopes of δD and $\delta^{18}O$ are ideal tracers for tracking various hydrogeochemical processes
38 (Liu et al., 2014). Dogramaci et al. (2012) studied the hydrogeochemical and isotopic characteristics of the
39 Hamersley Basin in northwestern Australia and provided a theoretical basis for the sustainable development of
40 local water resource utilization. The descriptive statistical method, the Piper diagram and the main ion component
41 proportion coefficient and factor analysis method were used to study hydrogeochemical characteristics of



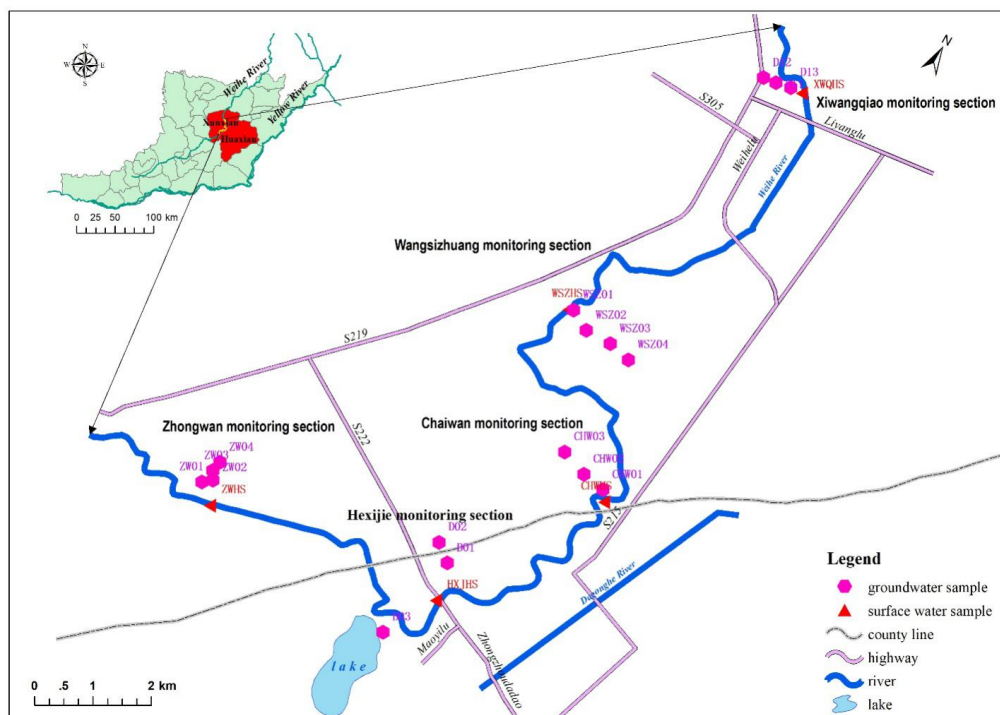
42 groundwater in the Sara Wusu aquifer system in the Ordos Basin (Yang et al., 2016). Fuzzy mathematics and
43 multivariate statistical methods were used to study the quality characteristics of surface water and groundwater in
44 the Songnen plain (Zhang et al., 2012). Zeng et al. (2013) studied the spatial distribution of hydrogeochemical and
45 isotopic characteristics of different water bodies, including spring water, river water and lake water, in different
46 parts of Tajikistan and discussed their origins and environmental significance. Although there are many studies
47 related to the chemical and isotopic characteristics of groundwater and surface water, the relationship between
48 surface water and groundwater transformation is still a prevalent topic in hydrology and water resource studies
49 (Wang et al., 2016; Lu et al., 2016b), hydrogeochemistry, biogeochemistry, and ecohydrology. Hydrogen and
50 oxygen stable isotopes ($\delta^{18}\text{O}$ and δD) and electrical conductivity (EC) were used to study the mutual relationship
51 among precipitation, river water and groundwater in Taiwan Douliushan (Peng et al., 2014). Multivariate
52 statistical analysis methods and isotope analysis methods were used to study the hydraulic linkage between
53 surface water and ground water and their temporal and spatial variation in the Condamine River in Australia
54 (Martinez et al., 2015). Hydrogen and oxygen isotopes were used to study the relationship of recharge and
55 discharge between the various water bodies on the Portuguese island of Madeira, from which a hydrogeological
56 conceptual model of Madeira Island was established (Prada et al., 2016). By analyzing the hydrogeochemical
57 characteristics of surface water and groundwater in the Heihe River Basin, Nie et al. (2005) identified the
58 transformation relationship between groundwater and surface water in the main stream of Heihe River. Hydrogen
59 and oxygen isotopes and water chemistry were used to investigate the relationship between surface water and
60 groundwater of the Second Songhua River, and the end element method was used to quantitatively calculate a
61 conversion proportion between surface water and groundwater (Zhang et al, 2014).

62 The surface water of Weihe River is seriously polluted and has become a major pollution source for nearby
63 shallow groundwater. This seriously affects the exploitation, utilization and protection of groundwater resources
64 and endangers the ecological safety and the health of the residents (Lu et al., 2016c). The surface water and
65 groundwater were sampled in several typical sections of the Weihe River Basin to study the conversion
66 relationship between surface water and groundwater based on the hydrogeochemical and isotopic characteristics
67 and to provide a basis for groundwater protection, restoration and management.

68 2. Materials and methods

69 2.1 Study area

70 The Weihe River Basin, which is 344.5 km long and has a basin area of 14970 km², is located in the northern
71 part of the Henan Province, south of the North China Plain. It is the main tributary to the Zhangweinan Canal,
72 which is a tributary to the Haihe River. The Weihe River Basin has a warm, temperate, continental monsoon
73 climate. It is cold, with minor rain in the winter, hot and rainy in the summer, and the average annual precipitation
74 in the basin is 608 mm (Zhu et al., 2006). The influence of river pollutants on groundwater is mainly banded and
75 has a relatively small area of influence. A 26.67-km-long segment of the Weihe River between Xizhangzhuang
76 village of Xiaohe Town and Dongwangqiao village of Liyang Town, considering the shallow groundwater along
77 both sides of the river, was selected as the study area. This is an area of approximately 160 km² (shown in Fig. 1).
78 The Weihe River Basin is closely related to groundwater, and the polluted river water of the Weihe River is a
79 pollution source of groundwater on both sides of the river. The groundwater is mainly supplied by atmospheric
80 precipitation, lateral seepage, piedmont lateral runoff and canal leakage, and drainage is dominated by artificial
81 extraction and evaporation. Groundwater flows from the southwest to the northeast, which is generally consistent
82 with the topography. The average hydraulic gradient is 1/3000.



83
 84

Fig. 1 The location of the study area and the distribution of sampled sections

85 **2.2 Sample collection**

86 According to the goals of the study, the surface water sampling sites were chosen parallel to the direction of
 87 river flow, and the groundwater sampling sites were chosen perpendicular to the river flow. There were 5 sections
 88 sampled from upstream to downstream between Xiaohe Town and Liyang Town along the Weihe River (i.e., the
 89 Zongwan sample section, Hexijie sample section, Chaiwan sample section, Wangsizhuang sample section and
 90 Xiwangqiao sample section). A total of 5 surface water samples and 17 groundwater samples were collected.
 91 Among them, ZWHS, HXJHS, CHWHS, WSZHS and XWQHS were surface water sampling sites, and the others
 92 were groundwater sampling sites. The samples were collected in May 2016. The sampling sites encompassed the
 93 band of influence of pollutants from the Weihe River on groundwater. The locations of the sampling sites and the
 94 types of water samples are shown in Figure 1.

95 Groundwater was sampled mainly from irrigation wells and drinking wells. Prior to sampling, wells were
 96 pumped for more than 20 min until the temperature, EC, and pH were stable. Surface water samples were
 97 collected from the river bank at a depth of more than 50 cm. Samples were collected in 500 ml polyethylene
 98 bottles, which were cleaned with sample water at least three times prior to sampling. When each sample was
 99 collected, no bubbles were left in the bottle, and the outer cap was sealed with sealant to prevent air exchange.
 100 Samples were brought back to the laboratory and stored in a refrigerated container at 0 to 4 °C.

101 **2.3 Stable hydrogen and oxygen isotopes and hydrogeochemical analysis**

102 Hydrogen and oxygen isotopes were measured in the laboratory of groundwater science and engineering of
 103 the Ministry of Land and Resources of the Institute of Hydrogeology and Environmental Geology at the Chinese



104 Academy of Geological Sciences. Analyses were conducted using wavelength scanning-optical cavity ring down
 105 spectroscopy. The ratio of hydrogen and oxygen isotopes (δ) is expressed as the deviation relative to Vienna
 106 VSMOW (Zhao, et al, 2015):

$$107 \quad \delta(\text{‰}) = \frac{R_{sp} - R_{st}}{R_{st}} \times 1000 \quad (1)$$

108 where R_{sp} and R_{st} refer to the ratio of D/H (or $^{18}\text{O}/^{16}\text{O}$) in samples and VSMOW, respectively. When δD and
 109 $\delta^{18}\text{O}$ are positive, the samples are enriched with D and ^{18}O compared to the VSMOW standard; when they are
 110 negative, the two isotopes are diluted compared to the VSMOW standard (Zhang et al., 2006).

111 Analyses of water chemistry components were completed in the laboratory of hydrogeology at the North
 112 China University of Water Resources and Electric Power. The analyses included Cl^- , SO_4^{2-} , Na^+ , K^+ , NH_4^+ , Mg^{2+} ,
 113 HCO_3^- , CO_3^{2-} and Ca^{2+} . Among these ions, HCO_3^- and CO_3^{2-} were detected using acid-base indicator titration, Ca^{2+}
 114 and Mg^{2+} were detected using EDTA titration, and the other ions were detected using ion chromatography. pH,
 115 TDS, RDO, conductivity, redox potential and other indicators were detected *in situ* with a PX.68-smarTROLL
 116 MP hand-held multi-parameter water quality detector.

117 2.4 Conversion ratio of surface water to ground water

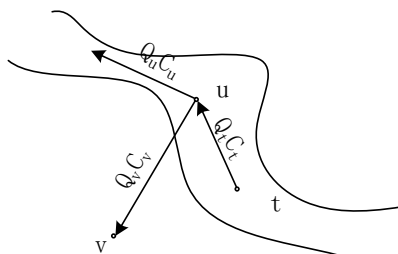
118 The stable hydrogen and oxygen isotope method can determine the sources of runoff, the division of river
 119 runoff and the conversion of surface water and groundwater. The principle of division is based on the mass
 120 conservation of isotopes (Song et al., 2007), in which the sum of two runoff components is equal to the flow of the
 121 resultant runoff, and the sum of the tracer flow of the two runoff components is equal to the sum of the tracer of
 122 synthetic runoff (Figure 2). The calculations are as follows:

$$123 \quad Q_t = Q_u + Q_v \quad (2)$$

$$124 \quad Q_t \cdot C_t = Q_u \cdot C_u + Q_v \cdot C_v \quad (3)$$

$$125 \quad f = \frac{Q_v}{Q_t} = \frac{C_t - C_u}{C_v - C_u} \quad (4)$$

126 where Q is the flux, C is the isotope component, t and u are surface water, and v is groundwater. f is the ratio
 127 of river water to ground water and is calculated with δD as a standard.



128
 129

Fig. 2 Principle diagram of the discharge hydrograph separation methods

130 **3. Results and discussion**131 **3.1 Characteristics of main hydrogeochemical components**

132 The water composition results are shown in Table 1. The groundwater pH in the study area was near neutral,
133 ranging from 6.83 to 7.81. The TDS ranged from 564.66 to 1747.84 mg/L, and the TDS of all 17 groundwater
134 samples exceeded the WHO drinking water standard of 500 mg/L. The relationship between the average
135 concentrations of groundwater anions was $\text{HCO}_3^- > \text{SO}_4^{2-} > \text{Cl}^-$. The concentration of HCO_3^- ranged from 461.75
136 mg/L to 735.15 mg/L, with an average concentration of 635.88 mg/L. The concentration of SO_4^{2-} ranged from
137 116.11 mg/L to 833.33 mg/L, with an average concentration of 307.52 mg/L. The concentration of Cl^- ranged
138 from 102.17 mg/L to 640.13 mg/L, with an average concentration of 275.24 mg/L. The relationship of the average
139 concentrations of the cations was $\text{Na}^+ > \text{Ca}^{2+} > \text{Mg}^{2+} > \text{K}^+$. Na^+ and Ca^{2+} were dominant, and their concentrations
140 ranged from 74.21 mg/L to 272.00 mg/L and 64 mg/L to 268.80 mg/L, respectively, with average values of
141 182.78 mg/L and 121.69 mg/L.

142 The pH of the Weihe River in the study area ranged from 8.03 to 8.22 and was therefore weakly alkaline.
143 The TDS ranged from 1401.32 to 1518.71 mg/L, which is generally higher than that of groundwater. The
144 relationships between the concentrations of anions and cations in surface water were $\text{SO}_4^{2-} > \text{Cl}^- > \text{HCO}_3^-$ and $\text{Na}^+ >$
145 $\text{Ca}^{2+} > \text{Mg}^{2+} > \text{K}^+$. The concentration of SO_4^{2-} in the river water ranged from 627.07 mg/L to 664.06 mg/L, with an
146 average value of 647.12 mg/L. The concentration of Cl^- ranged from 325.95 mg/L to 391.57 mg/L, with an
147 average concentration of 365.89 mg/L. The concentrations of Na^+ and Ca^{2+} ranged from 294.47 mg/L to 314.27
148 mg/L and 94.40 mg/L to 115.20 mg/L, respectively, and their mean values were 305.58 mg/L and 107.52 mg/L.
149 As seen in Table 1, there is no significant change in the ion concentration between the upstream and downstream
150 parts of the Weihe River.

151 According to WHO standard of drinking water, except for K^+ and pH, the other measured components of
152 surface water and groundwater all exceeded the maximum acceptable values in the study area. As such, both
153 surface water and groundwater along the Weihe River are not suitable drinking water sources.

154 **Table 1 Analytical results of water quality in the study area**

Ion content/ ($\text{mg}\cdot\text{L}^{-1}$)		pH	TDS	Na^+	K^+	Mg^{2+}	Ca^{2+}	Cl^-	SO_4^{2-}	HCO_3^-	TH
Groundwater (17)	Minimum	6.73	564.66	74.21	6.20	57.76	64.00	102.17	116.11	461.75	396.83
	Maximum	7.81	1747.84	272.00	34.26	162.38	268.80	640.13	833.33	735.15	1072.91
	Average	7.30	1170.00	182.78	16.58	110.23	121.69	275.24	307.52	635.88	756.18
Surface water (5)	Minimum	8.03	1401.32	294.47	24.23	49.90	94.40	325.95	627.07	282.52	480.13
	Maximum	8.22	1518.71	314.27	28.35	59.54	115.20	391.57	664.06	385.80	495.84
	Average	8.11	1473.74	305.58	26.40	53.79	107.52	365.89	647.12	350.56	489.33
WHO drinking water standards		6.5~8.5	500	200	100	30	75	200	200	200	100
Over-standard rate of groundwater (%)		0	100	47	0	100	70	70	65	100	100
Over-standard rate of surface water (%)		0	100	100	0	100	100	100	100	100	100

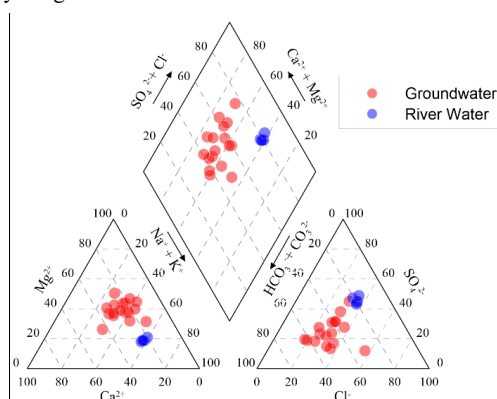
155

156 **3.2 Hydrogeochemical characteristics**

157 The Piper diagram is one of the most commonly used graphical methods for interpreting hydro-geological
158 problems. According to the analytical results, the Piper diagram of the hydrogeochemical composition of all water
159 samples in the study area is shown in Fig. 3. The results indicate that the chemical type of surface water in the
160 study area is the $\text{SO}_4\text{-Cl-Na}$ type, indicating that the surface water is uniform across the study area. From



161 upstream to downstream along the Weihe River, the water chemistry type of each groundwater section is as
162 follows: The Zong Wan section and Hexijie section are mainly HCO_3^- -Mg-Na types, the Chaiwan section is
163 mainly the $\text{SO}_4 \cdot \text{Cl}$ -Mg-Na type, the Wangsizhuang section is mainly the $\text{HCO}_3^- \cdot \text{SO}_4 \cdot \text{Cl}$ -Mg-Na type, and the
164 Xiwangqiao section is mainly the $\text{HCO}_3^- \cdot \text{Cl}$ -Mg-Ca-Na type. Usually, the chemical types of groundwater, from
165 the recharge area to the discharge area, change in the following ways: HCO_3^- — SO_4^{2-} — Cl^- . Considering the
166 chemical types of groundwater of each section, HCO_3^- is dominant in groundwater on both sides of river in the
167 upstream section, whereas SO_4^{2-} and Cl^- are dominant in the middle and lower reaches. The type of water
168 chemistry can indirectly verify the groundwater flow on both sides of river.



169
170

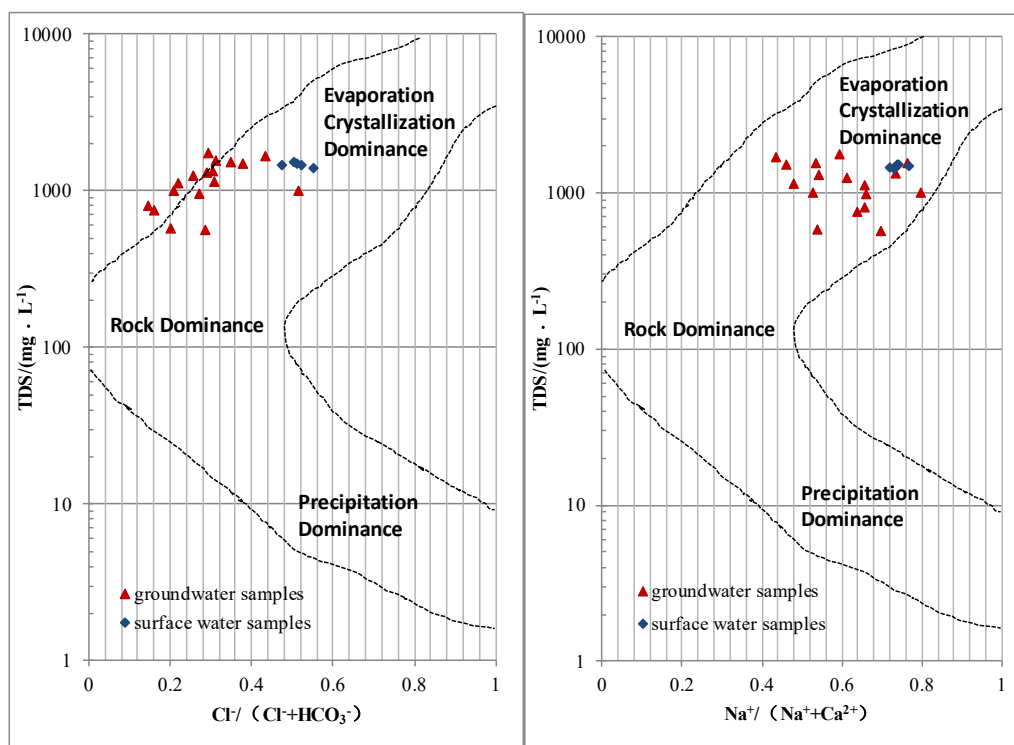
Fig. 3 Piper diagram of water chemistry for surface and groundwater in the study area

171 3.3 Analysis of formation function of water chemical composition

172 3.3.1 Analysis of formation function based on the Gibbs diagram

173 The Gibbs diagram can clearly indicate whether the chemical components of river and groundwater are the
174 precipitation dominance type, rock dominance type or evaporation crystallization dominance type. It is an
175 important way to qualitatively determine the effects of regional rocks, atmospheric precipitation, and evaporation
176 concentration on river water components (Wang et al., 2010). Generally, samples with low TDS and high
177 $\text{Na}^+ / (\text{Na}^+ + \text{Ca}^{2+})$ or $\text{Cl}^- / (\text{Cl}^- + \text{HCO}_3^-)$ ratios (close to 1) are mainly distributed in the lower-right corner, indicating
178 precipitation dominance. Samples with slightly high TDS and $\text{Na}^+ / (\text{Na}^+ + \text{Ca}^{2+})$ or $\text{Cl}^- / (\text{Cl}^- + \text{HCO}_3^-)$ ratios of
179 approximately 0.5 or less than 0.5 are mainly distributed in the middle zone, indicating rock dominance. Samples
180 with very high TDS and large $\text{Na}^+ / (\text{Na}^+ + \text{Ca}^{2+})$ or $\text{Cl}^- / (\text{Cl}^- + \text{HCO}_3^-)$ ratios are mainly distributed in the upper-right
181 corner, indicating evaporation crystallization dominance type, reflecting the influence of evaporation in arid areas
182 (Sun et al., 2014).

183 The ion concentrations of the 5 river groundwater samples and 17 groundwater samples from the study area
184 are shown on a Gibbs diagram in Fig. 4. It is apparent that the surface water in the study area is located the upper-
185 right corner of the diagram with a $\text{Na}^+ / (\text{Na}^+ + \text{Ca}^{2+})$ or $\text{Cl}^- / (\text{Cl}^- + \text{HCO}_3^-)$ ratio greater than 0.5 and with a high
186 content of TDS, indicating that surface water has an evaporation crystallization dominance origin. The
187 groundwater samples differ in the two figures but are mainly distributed in the evaporation crystallization
188 dominance region, slightly toward the rock dominance region, indicating that the chemical composition of water
189 is controlled by evaporation crystallization and rock weathering.



190

191

Fig. 4 Gibbs plots of the surface and groundwater chemistry in the study area

192 3.3.3 Analysis of formation function based on multivariate statistics

193 To further analyze the hydrogeochemical formation functions, factor analysis and R cluster analysis were
 194 performed on water samples using TDS, Cl^- , SO_4^{2-} , HCO_3^- , Na^+ , K^+ , Ca^{2+} , and Mg^{2+} as the original parameters.
 195 Seventeen groups of groundwater samples and 5 groups of surface water samples were calculated. After the
 196 calculation, the KMO value of the groundwater sample was 0.596. According to the KMO test standard, when
 197 $0.5 < \text{KMO} < 0.6$, the original variable is barely suitable for factor analysis. According to the calculation results
 198 (Table 2), the formation function of the groundwater chemical composition can be summarized in 3 factors, and
 199 the cumulative contribution rate of the 3 factors is 75%. The Ca^{2+} , Cl^- , SO_4^{2-} and TDS of factor 1 have higher
 200 positive load and the coefficient of Ca^{2+} and SO_4^{2-} is large, indicating that there may be weathering of calcium
 201 feldspar, dissolution of gypsum, or oxidation of pyrite. A large coefficient of Cl^- indicates that there may be
 202 leaching of halite. The Na^+ , Mg^{2+} and HCO_3^- of factor 2 have higher positive loads, which indicates possible
 203 weathering of carbonate or silicate. The alternating adsorption of cations between Na^+ and Ca^{2+} causes the content
 204 of Na^+ to increase. The K^+ content of factor 3 is large, which indicates possible weathering of feldspar. Surface
 205 water samples can be summarized in 2 factors, and the contribution rate of the 2 factors is 91%. The K^+ , HCO_3^-
 206 and TDS of factor 1 have higher positive loads, indicating the possible weathering of carbonate and feldspar. The
 207 Mg^{2+} , Na^+ and Cl^- of factor 2 have a higher positive load, which indicates the possible dissolution of halite and the
 208 alternate adsorption of cations between Na^+ and Ca^{2+} , which causes the content of Na^+ to increase.

209 Cluster analysis can be simplified as the identification of the relationship between large-scale samples. R
 210 cluster analysis is used to classify variables, and Q cluster analysis is used to classify samples (Sun and Gui,



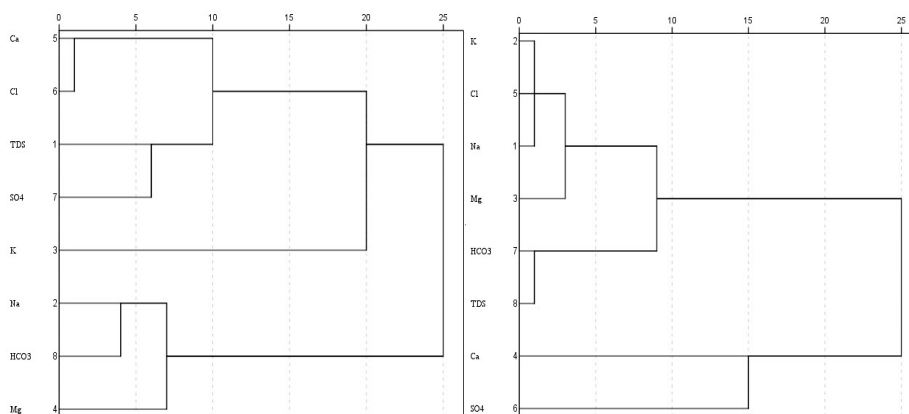
211 2013). The results of the R cluster analysis are shown in Figure 5. The groundwater components can be divided
 212 into 3 groups, which is consistent with the results of the factor analysis. The first group includes Ca^{2+} , Cl^- , SO_4^{2-}
 213 and TDS. The second group includes Na^+ , Mg^{2+} and HCO_3^- . Finally, the third group includes K^+ . Surface water
 214 ions can be divided into 2 groups. The first group includes TDS, Cl^- , HCO_3^- , Na^+ , K^+ and Mg^{2+} , and the second
 215 group includes Ca^{2+} and SO_4^{2-} . This indicates the presence of gypsum dissolution, which differs from the results
 216 of factor analysis.

217 In summary, a variety of complex hydrogeochemical processes may have occurred in the study area, such as
 218 concentration through evaporation, rock weathering, cation alternate adsorption, oxidation and dissolution.

219

Table 2 Factor analysis composition coefficient of ground and surface water

Parameter variable	Groundwater			Surface water	
	Factor 1	Factor 2	Factor 3	Factor 1	Factor 2
Ca^{2+}	0.889	-0.083	0.339	0.206	-0.970
Na^+	0.261	0.799	-0.041	0.650	0.738
K^+	0.061	0.081	0.916	0.783	0.540
Mg^{2+}	0.298	0.702	0.265	0.106	0.986
Cl^-	0.735	0.259	0.323	0.479	0.817
SO_4^{2-}	0.760	0.299	-0.046	-0.883	0.351
HCO_3^-	-0.004	0.915	0.010	0.812	0.151
TDS	0.762	0.197	-0.208	0.972	0.200
Characteristic value	3.472	1.492	1.037	4.856	2.446
Contribution rate%	43.394	18.649	12.965	60.704	30.578
Cumulative contribution rate	43.394	62.043	75.008	60.704	91.282



220

221

Fig. 5 R type cluster analysis

222 3.4 Isotopic characteristics and transformation relationships of surface water and groundwater

223 3.4.1 Isotopic variation characteristics

224 δD and $\delta^{18}\text{O}$ of surface water and groundwater and the d value of deuterium excess in the study area are
 225 listed in Table 3, in which $d = \delta\text{D} - 8\delta^{18}\text{O}$.

226 As seen in Table 3, δD and $\delta^{18}\text{O}$ of surface water are more enriched than in groundwater. The variation in δD
 227 and $\delta^{18}\text{O}$ for water from the Weihe River is small. $\delta^{18}\text{O}$ ranges from -7.8‰ to -7.6‰ with an average value of $-$



228 7.7‰, and δD ranges from -59‰ to -57‰ with an average value of -58‰. The range of $\delta^{18}O$ for shallow
229 groundwater is from -9.4‰ to -7.7‰, with an average value of -8.55‰; the range of δD is from -59‰ to -69‰,
230 with an average value of -63.3‰. The d value of deuterium excess of water is positive and less than 10 of the
231 atmospheric precipitation intercept. That of surface water is less than that of shallow groundwater, indicating that
232 the recharge sources of surface water and groundwater are subject to evaporation effects but that shallow
233 groundwater is less influenced by evaporation effects.

234 Generally, the isotopic characteristics of river water bodies increase from upstream to downstream because
235 of the isotopic fractionation that is caused by the evaporation of water. The closer to the lower reaches of the river,
236 the greater the fractionation effect is on the isotopes (Liu et al., 2014). Figure 6 shows the variation in δD and
237 $\delta^{18}O$ in river water. It is apparent that δD and $\delta^{18}O$ become more enriched as the river flows downstream, in which
238 $\delta^{18}O$ declines in HXJHS, probably because there is a lake in the vicinity of the upstream reaches and river water
239 supplies the lake.

240 For groundwater, the values of δD and $\delta^{18}O$ in the Zongwan section, Hexijie section and Xiwangqiao section
241 become more depleted as the distance between sampling points and Weihe River increases. The closer the sample
242 location is to the river, the closer the δD and $\delta^{18}O$ values are to the surface water, indicating that the influence of
243 surface water on groundwater decreases with increasing distance. In contrast, the influence of precipitation and
244 irrigation infiltration recharge on groundwater is enhanced. The values of δD and $\delta^{18}O$ for the Chaiwan section
245 and the Wangsizhuang section become enriched as the distance between the sampling points and the Weihe River
246 increases. This is likely because the farmland in the Chaiwan section and the Wangsizhuang section is mainly
247 irrigated using Weihe River water, and the infiltration of irrigation water causes the enrichment of hydrogen and
248 oxygen isotopes in the groundwater. The hydrogen and oxygen isotope characteristics are more similar to those of
249 the Weihe River. The CHW02 and CHW03 sampling points in the Chaiwan section are located in an area affected
250 by river irrigation, and CHW01 is a household well. As such, the hydrogen and oxygen isotope values are
251 $CHW03 \geq CHW02 > CHW01$. Similarly, WSZ02, WSZ03 and WSZ04 in the Wangsizhuang section are located in
252 an area affected by river irrigation, and WSZ01 is a household well. Thus, $WSZ04 \geq WSZ03 \geq WSZ02 > WSZ01$.

253

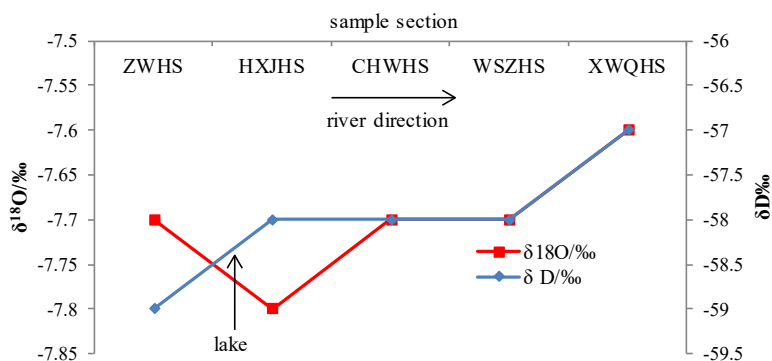
Table 3 δD , $\delta^{18}O$ and d values of water samples in study area

Water sample type	No.	$\delta D/\text{‰}$	$\delta^{18}O/\text{‰}$	$d/\text{‰}$	$f/\text{‰}$
Surface water	ZWHS	-59	-7.7	2.6	
	HXJHS	-58	-7.8	4.4	
	CHWHS	-58	-7.7	3.6	
	WSZHS	-58	-7.7	3.6	
	XWQHS	-57	-7.6	3.8	
	average	-58	-7.7	3.6	
Shallow groundwater	ZW01	-62	-8.6	6.8	33.3
	ZW02	-63	-8.6	5.8	25
	ZW03	-63	-8.6	5.8	25
	ZW04	-69	-9.4	6.2	10
	D01	-65	-8.7	4.6	14.3
	D02	-66	-8.9	5.2	12.5
	D03	-60	-8	4	50
	CHW01	-63	-8.6	5.8	20
	CHW02	-62	-8.4	5.2	25
	CHW03	-62	-8.3	4.4	25



WSZ01	-68	-9.2	5.6	10
WSZ02	-63	-8.6	5.8	20
WSZ03	-63	-8.5	5	20
WSZ04	-63	-8.5	5	20
D11	-59	-7.7	2.6	50
D12	-62	-8.4	5.2	20
D13	-63	-8.4	4.2	16.7
Average	-63.3	-8.55	5.1	

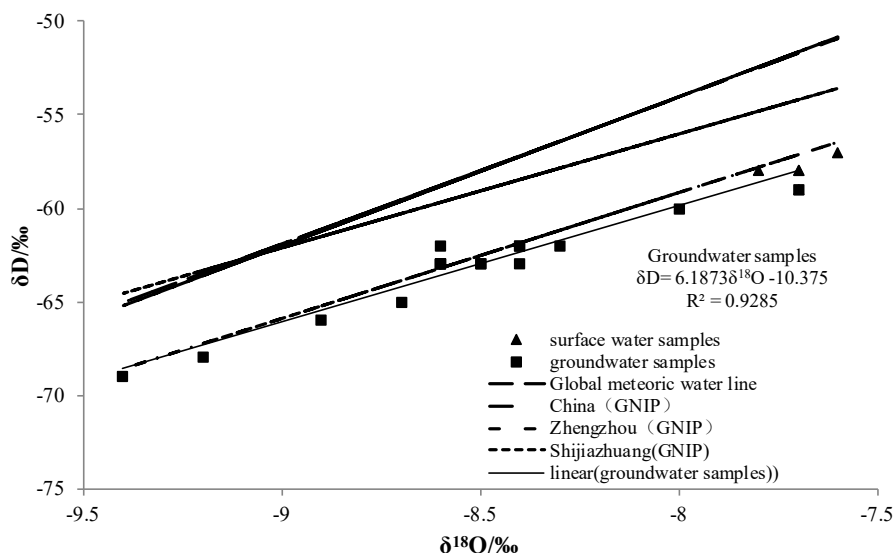
254



255

256

Fig. 6 Isotopic variation of surface water



257

258

Fig. 7 Relationship between δD and $\delta^{18}O$ of surface water and groundwater

259

260

261

262

According to the 27 GNIPs set up in China by the International Atomic Energy Association (IAEA), the monitoring sites that are closest to the study area are at Shijiazhuang and Zhengzhou. The meteoric water line $\delta D = 6.75 \delta^{18}O - 5.12$ in Zhengzhou is close to the characteristic line for hydrogen and oxygen isotopes of samples in the study area (Figure 7), so the meteoric water line in Zhengzhou is assumed to be the local meteoric water



263 line (LMWL). When the compositions of δD and $\delta^{18}O$ of water samples are compared to the meteoric water line,
264 the source of the local river water and shallow groundwater and their mutual transformation relationship can be
265 distinguished. From drawing the trend line between the underground water sample points, the relationship
266 between δD and $\delta^{18}O$ is $\delta D = 6.1873\delta^{18}O - 10.375$, and the correlation coefficient is 0.9285. From drawing the trend
267 line between the groundwater and surface water sample points, the relationship between δD and $\delta^{18}O$ is
268 $\delta D = 6.19328\delta^{18}O - 10.321$, and the correlation coefficient is 0.9585. The two trend lines are basically the same, and
269 the related coefficient is very high. The surface water sample points are located in the direction of the
270 groundwater trend line that extends to the right. δD and $\delta^{18}O$ are relatively enriched, indicating that the sources of
271 surface water and groundwater are the same and that there is a hydraulic connection. The hydraulic connection
272 between the two is a single-line infiltration of the surface river water into groundwater. The trend line is close to
273 the local meteoric water line (LMWL) and the slope is small, indicating that surface water and groundwater are
274 recharged from meteoric water but are also subject to the evaporation, resulting in the enrichment of hydrogen and
275 oxygen isotopes.

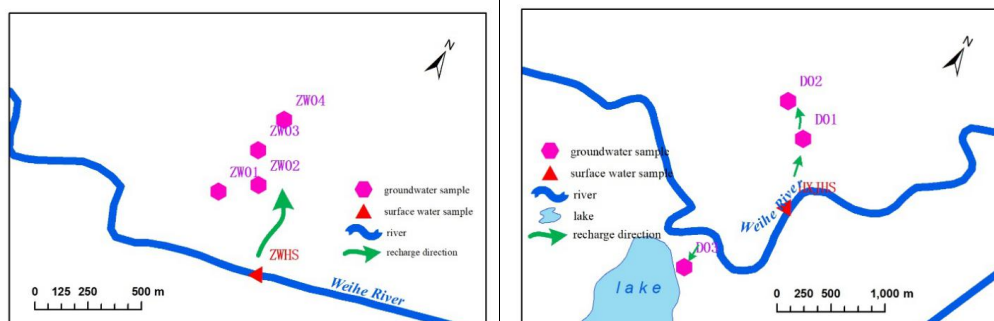
276 3.4.2 Estimation of recharge capacity of river water to groundwater

277 According to the stable isotope signatures of the water samples, the calculated results of ratio f of
278 groundwater recharge to river water are shown in Table 4. The ratio f of surface water infiltration to recharge
279 groundwater in each observation section has a different, but regular, pattern, and the results are shown in Figure 8.

280 In the Zongwan section (Figure 8a), as the distance between groundwater sampling sites and the river
281 increased (ZW01 toward ZW04), the ratio of surface water infiltration to groundwater recharge (f) decreased from
282 33.3% to 10%, indicating that the river water recharges groundwater in this section and the direction of
283 groundwater flow is from ZW01 toward ZW04. The infiltration rates at D01 and D02 in the Hexijie section
284 (Figure 8b) are 14.3% and 12.5%, respectively, with a decreasing trend, indicating that there is a small amount of
285 river water recharging groundwater in that section, with a direction of groundwater flow from D01 toward D02.
286 The ratio of surface water infiltration to groundwater at D03 is as high as 50%, indicating that the river mainly
287 recharges the artificial lake that exists near D03 in the Hexijie section. The ratio of surface water infiltration to
288 groundwater in the Chaiwan section (Figure 8c) increases from 20% to 25% as the distance increases between
289 groundwater sampling sites and the river, whereas it increases from 10% to 20% in the Wangsizhuang section
290 (Figure 8d). This may be associated with the unique river trend of the two sections. The Chaiwan section and the
291 Wangsizhuang section are located near the right corner of the river, where the influence of the river water on
292 groundwater is complicated, but the river is the main supplier of groundwater. The groundwater flow line is the
293 closed space where water is not exchanged with the outside world. Some input values remain constant along the
294 entire streamline, such as δD and $\delta^{18}O$. Therefore, it is possible to interpret that WSZ01, WSZ02, and WSZ03 are
295 on the same streamline. At the same time, because farmland is primarily irrigated by water from the Weihe River,
296 irrigation water infiltrates the soil to recharge groundwater, resulting in the enrichment of hydrogen and oxygen
297 isotopes. For the Xiwangqiao section (Figure 8e), the ratio of river water infiltration to groundwater at D11 is
298 close to 50%, whereas it is 20% and 16.7% at D12 and D13, respectively. This is primarily because D11 is located
299 in the convexity of the river, where it is significantly eroded with a large amount of infiltration.



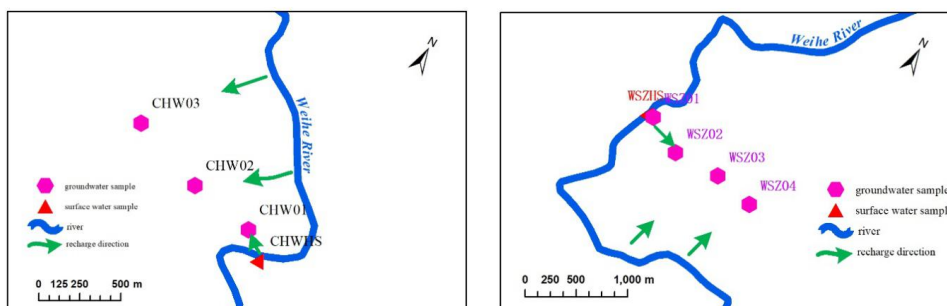
300
 301



(a) Zongwan section

(b) Hexijie section

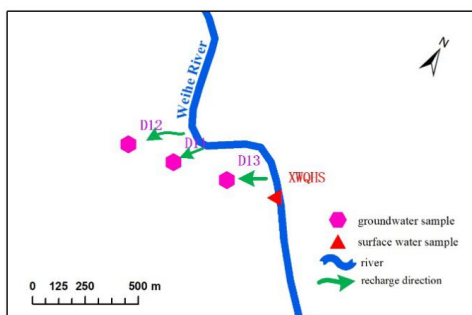
302
 303



(c) Chaiwan section

(d) Wangsizhuang section

304
 305



(e) Xiwangqiao section

306 **Fig. 8 Relationships between surface water and groundwater**

307 **4. Conclusions**

308 The surface water components of Weihe River display no significant spatial variation, but the ion
 309 concentrations of groundwater samples from 5 sections are different. The cation concentrations of surface water
 310 and groundwater are consistent, with $\text{Na}^+ > \text{Ca}^{2+} > \text{Mg}^{2+} > \text{K}^+$. The relative concentrations of anions in groundwater
 311 are $\text{HCO}_3^- > \text{SO}_4^{2-} > \text{Cl}^- > \text{NO}_3^-$, whereas the relative concentrations of anions in the surface water are $\text{SO}_4^{2-} > \text{Cl}^- >$
 312 $\text{HCO}_3^- > \text{NO}_3^-$. The surface water in all sections of the Weihe River is the $\text{SO}_4\text{-Cl-Na}$ type, whereas the
 313 hydrogeochemical types of groundwater are different. HCO_3^- dominates in the groundwater in the upper reaches



314 of the river, and SO_4^{2-} and Cl^- dominate in the middle and lower reaches.

315 By using a Gibbs diagram, factor analysis and cluster analysis, we established that the geochemical processes
316 of the Weihe River Basin include concentration by evaporation, rock weathering, cation alternate adsorption and
317 dissolution. Because surface water is an open system, the source of ions in a water body is greatly influenced by
318 human activity and atmospheric precipitation, whereas the factors contributing to the formation of water
319 chemistry are more complex.

320 The isotope results show that δD and $\delta^{18}\text{O}$ of the surface water in the Weihe River varies little and is more
321 enriched than the groundwater is. The shallow groundwater at different sections is affected by rainfall, irrigation,
322 river recharge and evaporation, resulting in different δD and $\delta^{18}\text{O}$ values. By analyzing hydrogen and oxygen
323 isotopic characteristics of surface water and groundwater in different sections and using the segmentation of flow
324 duration curve, it was established that surface water recharges groundwater at 5 sections along the Weihe River,
325 and each section has unique recharge intensity and relationship due to its unique hydraulic environment.

326 Due to the lack of local isotope monitoring data for meteoric water, the Zhengzhou meteoric water line was
327 used to analyze the isotopic characteristics of surface water and groundwater. The existing household wells were
328 used as groundwater sampling points. Because they are affected by towns and villages surrounding the Weihe
329 River, groundwater sampling points cannot be fully symmetric and isometric relative to the Weihe River. As such,
330 the research results need to be improved by monitoring more complete data in future research.

331 Acknowledgments

332 The study was financially supported by Non-Profit Industry Specific Research Projects of Ministry of Water
333 Resources, China, Grant NO: 201401041 and 201501008, the Open Research Fund of State Key Laboratory of
334 Simulation and Regulation of Water Cycle in River Basin (China Institute of Water Resources and Hydropower
335 Research), Grant NO: IWHR-SKL-201208, and Science and Technology Research Key Project of the Education
336 Department of Henan Province, Grant NO: 14A170006.

337 References

- 338 [1] B. Zhang, X. Song, Y. Zhang, D. Han, C. Tang, Y. Yu, Y. Ma. 2012. Hydrochemical characteristics and water quality
339 assessment of surface water and groundwater in Songnen plain, Northeast China, *Water Research*, 46 (8): 2737-2748.
- 340 [2] B. Zhang, X. Song, Y. Zhang, D. Han, L. Yang, C. Tang. 2014. Relationship between surface water and groundwater in the
341 second Songhua River basin, *Advances in Water Science*, 25 (3): 336-347.
- 342 [3] F. Liu, S. Wang, Y. Lan, X. Hu. 2014. Environmental isotopes and exchanges of surface water-groundwater system in the
343 Zhangye basin of Heihe River watershed, *South-to-North Water Transfers and Water Science & Technology*, 12 (2): 92-96.
- 344 [4] H. Zeng, J. Wu. 2013. Water isotopic and hydrochemical characteristics and causality in Tajikistan, *Advances in Water
345 Science*, 24 (2): 272-279.
- 346 [5] J.H. Wang, S.B. Lu, L. Pei. 2016. Study on rules of dynamic variation of nitrogen in soil after reclaimed water drip irrigation,
347 *International Journal of Hydrogen Energy*, 41(35):15938-15943.
- 348 [6] J.L. Martinez, M. Raiber, M. E. Cox. 2015. Assessment of groundwater-surface water interaction using long-term
349 hydrochemical data and isotope hydrology: Headwaters of the Condamine River, Southeast Queensland, Australia, *Science of
350 the Total Environment*, 536: 499-516.
- 351 [7] L. Sun, H. Gui. 2013. Statistical analysis of deep groundwater geochemistry from Taoyuan Coal Mine, northern Anhui
352 Province, *Journal of China Coal Society*, 38 (s2): 442-447.
- 353 [8] P. B. Chattopadhyay, V. S. Singh. 2013. Hydrochemical evidences: Vulnerability of atoll aquifers in Western Indian Ocean to
354 climate change, *Global & Planetary Change*, 106: 123-140.
- 355 [9] P. Sun, Q. Yi, G. Xu. 2014. Characteristics of water chemistry and their influencing factors in subsidence waters in the Huainan



- 356 and Huaibei mining areas, Anhui Province, *Journal of China Coal Society*, 39 (7) :1345-1353.
- 357 [10] Q. Yang, L. Wang, H. Ma, K. Yu, J. D. Martin. 2016. Hydrochemical characterization and pollution sources identification of
358 groundwater in Salawusu aquifer system of Ordos Basin, China, *Environmental Pollution*, 216: 340-349.
- 359 [11] R. Ma, Q. Dong, Z. Sun, C. Zheng. 2013. Using heat to trace and model the surface water-groundwater interactions: a review,
360 *Geological Science and Technology Information*, 32 (2): 131-137.
- 361 [12] S. Dogramaci, G. Skrzypek, W. Dodson, P. F. Grierson. 2012. Stable isotope and hydrochemical evolution of groundwater in
362 the semi-arid Hamersley Basin of subtropical northwest Australia, *Journal of Hydrology*, 475 (26): 281-293.
- 363 [13] S. Prada, J. V. Cruz, C. Figueira. 2016. Using stable isotopes to characterize groundwater recharge sources in the volcanic
364 island of Madeira, Portugal, *Journal of Hydrology*, 536: 409-425.
- 365 [14] S. Zhao, S. Pang, R. Wen, Z. Liu. 2015. Influence of below-cloud secondary evaporation on stable isotope composition in
366 precipitation in the Haihe River Basin, China, *Progress in Geography*, 34 (8):1031-1038.
- 367 [15] S.B. Lu, H.J. Bao, H.L. Pan. 2016c. Urban water security evaluation based on similarity measure model of Vague sets,
368 *International Journal of Hydrogen Energy*, 41(35):15944-15950.
- 369 [16] S.B. Lu, J.H. Wang, L. Pei. 2016b. Study on the Effects of Irrigation with Reclaimed Water on the Content and Distribution of
370 Heavy Metals in Soil, *International Journal of Environmental Research & Public Health*, 13(3):298.
- 371 [17] S.B. Lu, L. Pei, X. Bai. 2015. Study on method of domestic wastewater treatment through new-type multi-layer artificial
372 wetland, *International Journal of Hydrogen Energy*, 40(34):11207-11214.
- 373 [18] S.B. Lu, X.L. Zhang, H.J. Bao, M. Skitmore. 2016a. Review of social water cycle research in a changing environment,
374 *Renewable & Sustainable Energy Reviews*, 63:132-140.
- 375 [19] T. Keesari, K.L. Ramakumar, S. Chidambaram, S. Pethperumal, R. Thilagavathi. 2016. Understanding the hydrochemical
376 behavior of groundwater and its suitability for drinking and agricultural purposes in Pondicherry area, South India – A step
377 towards sustainable development, *Groundwater for Sustainable Development*, 2-3: 143-153.
- 378 [20] T. Peng, W. Lu, K. Chen, W. Zhan, T. Liu. 2014, Groundwater-recharge connectivity between a hills-and-plains' area of
379 western Taiwan using water isotopes and electrical conductivity, *Journal of Hydrology*, 517: 226-235.
- 380 [21] X. Song, X. Liu, J. Xia, J. Yu, C. Tang. 2007. A study of interaction between surface water and groundwater using
381 environmental isotopes in Huaisha River basin, *Science in China (Series D)*, 37 (1): 102-110.
- 382 [22] X. Zhu, Z. Wang, J. Li, L. Yu, J. Wang. 2006. Applications of SWAT model in Zhang Wei River Basin, *Progress in
383 Geography*, 25 (5): 106-111.
- 384 [23] Y. Wang, L. Wang, C. Xu, J. Ji, X. Xia, Z. An, J. Yuan. 2010. Hydro-geochemistry and genesis of major ions in the Yangtze
385 River, China, *Geological Bulletin of China*, 29 (2-3): 446-456.
- 386 [24] Y. Zhang, Y. Wu, X. Wen, J. Su. 2006. Application of environmental isotopes in water cycle, *Advances in Water Science*, 17
387 (5):738-747.
- 388 [25] Y.Z. Shang, S.B. Lu, X.F. Li, P.F. Hei, X.H. Lei, J.G. Gong, J.H. Liu, J.Q. Zhai, H. Wang. 2017. Balancing development of
389 major coal bases with available water resources in China through 2020, *Applied Energy*, 194:735-750.
- 390 [26] Z. Nie, Z. Chen, X. Chen, M. Hao, G. Zhang. 2005. The chemical information of the interaction of unconfined groundwater
391 and surface water along the Heihe River, Northwestern China, *Journal of Jilin University(Earth Science Edition)*, 35(1): 48-51.